

Isotope effect on the lifetime of the $2p_0$ state in phosphorus-doped silicon

H.-W. Hübers,^{1,2,*} S. G. Pavlov,¹ S. A. Lynch,³ Th. Greenland,⁴ K. L. Litvinenko,⁵ B. Murdin,⁵ B. Redlich,⁶ A. F. G. van der Meer,⁶ H. Riemann,⁷ N. V. Abrosimov,⁷ P. Becker,⁸ H.-J. Pohl,⁹ R. Kh. Zhukavin,¹⁰ and V. N. Shastin¹⁰

¹*Institute of Planetary Research, German Aerospace Center (DLR), Rutherfordstrasse 2, 12489 Berlin, Germany*

²*Institut für Optik und Atomare Physik, Technische Universität Berlin, Straße des 17. Juni 135, 10623 Berlin, Germany*

³*School of Physics and Astronomy, Cardiff University, Cardiff CF24 3AA, United Kingdom*

⁴*London Centre for Nanotechnology, University College London, 17–19 Gordon Street, London WC1H 0AH, United Kingdom*

⁵*Advanced Technology Institute, University of Surrey, Guildford GU2 7XH, United Kingdom*

⁶*Institute for Molecules and Materials, Radboud University Nijmegen, Heyendaalseweg 135, 6500 GL Nijmegen, the Netherlands*

⁷*Leibniz Institute of Crystal Growth, Max-Born-Straße 2, 12489 Berlin, Germany*

⁸*Physikalisch Technische Bundesanstalt, 38116 Braunschweig, Germany*

⁹*VITCON Projectconsult GmbH, 07743 Jena, Germany*

¹⁰*Institute for Physics of Microstructures, Russian Academy of Sciences, 603950 Nizhny Novgorod, Russia*

(Received 22 April 2013; revised manuscript received 5 June 2013; published 2 July 2013)

The low-temperature (~ 5 K) phonon-assisted relaxation of the $2p_0$ state of phosphorus donors in isotopically pure, monocrystalline ^{28}Si has been studied in the time domain using a pump-probe technique. The lifetime of the $2p_0$ state in $^{28}\text{Si}:\text{P}$ is found to be 235 ps, which is 16% larger than the lifetime of a reference $\text{Si}:\text{P}$ sample with a natural isotope composition. The interaction of the $2p_0$ state with intervalley g -type longitudinal acoustic and f -type transverse acoustic phonons determines its lifetime. This interaction, which depends on the homogeneity of the crystal, becomes weaker in ^{28}Si because of its more perfect crystal lattice compared to natural Si, and this leads to a longer lifetime. The difference between the linewidths of the $1s(A_1) \rightarrow 2p_0$ transition in $^{28}\text{Si}:\text{P}$ and natural $\text{Si}:\text{P}$ is more than a factor of two. It follows that linewidth broadening due to isotopic composition is an inhomogeneous process.

DOI: [10.1103/PhysRevB.88.035201](https://doi.org/10.1103/PhysRevB.88.035201)

PACS number(s): 71.55.Cn, 78.47.da

I. INTRODUCTION

Silicon (Si) is the most widely used and the most important semiconductor. Despite many experimental and theoretical investigations, the lifetimes of excited states in n - and p -type-doped Si remain a puzzle. These lifetimes have been determined for a number of dopants and excited states either by direct time-domain measurements^{1,2} or from the linewidths of transitions in absorption spectra.³ However, theoretical understanding is still lacking. For example, the lifetime of the $2p_0$ state in Si doped by phosphorus ($\text{Si}:\text{P}$) has been measured as 205 ps (Ref. 1), while models predict lifetimes of 40 ps or 1.1 ns.^{4,5} This indicates that the interaction of the donor electron with the host lattice is not fully understood. In addition, several exciting applications rely on transitions between states of group V donors in Si. These include using shallow donors embedded in a Si matrix as active elements in qubits for quantum computing and spintronics,^{6–9} terahertz lasers operating on donor optical transitions,¹⁰ and terahertz Raman lasers.¹¹ All of these applications require a detailed understanding of the lifetimes of excited states.

So far, most investigations have been done on Si crystals with natural isotopic composition ($^{\text{nat}}\text{Si}$). In this paper, we focus on high-quality, isotopically enriched $^{28}\text{Si}:\text{P}$ crystals. These crystals are an excellent material for fundamental investigations, since their structure is almost perfect.¹² Because of their perfection, such ^{28}Si crystals are a promising candidate for the new definition of the kilogram.¹³ Although the composition of natural Si (92.23% ^{28}Si , 4.67% ^{29}Si , and 3.1% ^{30}Si) is close to that of monoisotopic ^{28}Si , the isotopic composition can significantly influence the material properties. Some examples are the thermal conductivity, which increases

by a factor of eight in ^{28}Si (Ref. 14); the heat capacity, which increases with isotopic mass¹⁵; the lattice parameter, which decreases with isotopic mass¹⁶; the band gaps of Si (Ref. 17); the energy structure and optical transitions of impurity centers in Si (Ref. 3); and the phononic spectra.¹⁸

In this paper, we report on direct lifetime measurements of the $2p_0$ state in phosphorus-doped, isotopically enriched ^{28}Si using a terahertz pump-probe technique on the $1s(A_1) \rightarrow 2p_0$ transition. We carried out the same measurements with phosphorus-doped $^{\text{nat}}\text{Si}$. By comparing the results, we are able to study the influence of isotopic composition on the lifetime of the $2p_0$ state.

II. ENERGY LEVELS OF GROUP V DONORS IN SILICON

The energy levels of group V donors in Si are special, because the sixfold degeneracy of donor states is partially lifted because of valley-orbit interaction. Effective mass theory (EMT) is not sufficient to describe the donor binding energy correctly, because the wave functions of the symmetric s -type states have significant amplitudes close to the donor ion, where the coulomb potential is less screened. This causes splitting (also called chemical splitting), and a downshift in energy of the s levels, which is most pronounced for the $1s$ ground state (Fig. 1(a)).¹⁹ The $1s$ state splits into $1s(A_1)$ singlet, $1s(T_2)$ triplet, and $1s(E)$ doublet states, with the $1s(E)$ and $1s(T_2)$ states close to what is predicted by EMT and the $1s(A_1)$ ground state significantly lower. The decay of an electron is controlled by phonon-assisted relaxation and at a low temperature strongly depends on the energy gap to the nearest lower state. The relatively large energy gaps between the lowest excited

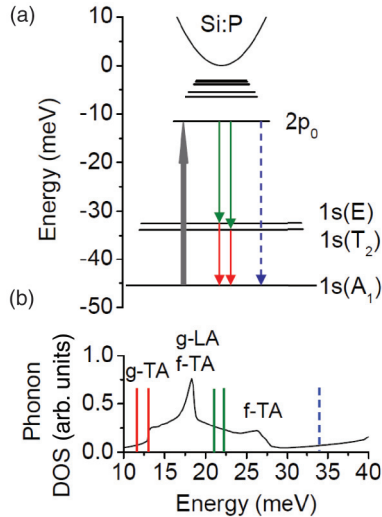


FIG. 1. (Color online) (a) Energy levels of Si:P (Ref. 19). The bold upward arrow indicates the pump transition. The downward arrows indicate the possible decay paths. The green and red straight arrows mark the path with the largest rate, while the dashed blue arrow indicates the direct decay into the ground state. (b) Phonon density of states (DOS) (Ref. 20). The lines indicate the positions of the transitions shown in (a). The interaction with the g -LA and f -TA phonons at 18 meV is the process that dominates the decay from the $2p_0$ state. The g -TA phonon is in resonance with the $1s(E)$, $1s(T_2) \rightarrow 1s(A_1)$ transitions.

donor states affect the decay times of these states such that they are relatively long lived. For Si:P, the lowest p -type state, $2p_0$, has the largest energy gap to the lower $1s(E)$ and $1s(T_2)$ donor states and therefore the longest lifetime in comparison with other odd parity states. This effect makes Si doped by group V donors, and in particular the $2p_0$ state in Si:P, attractive for terahertz lasers and optical manipulation of impurity states. When considering the lifetime of the $2p_0$ state and the decay of electrons into the $1s(A_1)$ state, one has to consider the intermediate states $1s(E)$ and $1s(T_2)$. In the case of Si:P electrons, which are captured in the $2p_0$ state, there are essentially two ways to reach the $1s(A_1)$ ground state: the electrons either decay directly into the $1s(A_1)$ state or undergo a two-step process—a first decay into one of the split-off $1s$ states, followed by a second decay into the ground state [Fig. 1(a)]. Theoretical estimates show that the indirect path via the split-off states is the dominant process. Electrons first decay into the $1s(E)$ and $1s(T_2)$ states by emission of intervalley g -type longitudinal acoustic (g -LA) and f -type transverse acoustic (f -TA) phonons. By emission of g -TA phonons, they further decay into the $1s(A_1)$ ground state. The latter step is a much faster process,²¹ because the g -TA phonon is in resonance with the $1s(E), 1s(T_2) \rightarrow 1s(A_1)$ transitions [Fig. 1(b)]. From the symmetry of the donor states, it follows that intravalley scattering from the $1s(T_2)$ state into the ground state is not allowed.²²

In principle, the lifetime of a state can be indirectly inferred from the absorption linewidth of an impurity transition involving this state—provided that the line is predominantly lifetime (homogeneously) broadened. In practice, this is challenging, because the measured absorption linewidth is a convolution of the natural, homogeneous linewidth; the instrument response;

and various inhomogeneous broadening effects. The most important ones are Stark broadening from random electric fields, concentration broadening due to overlap of excited state wave functions, and strain broadening. They are caused by impurities and lattice defects. Recently isotopic broadening has been identified as another inhomogeneous broadening mechanism.²³ Because of its larger extent, the excited state donor wave function samples a larger region of the crystal than does the more confined ground state and thus always samples a distribution of isotopes close to the average. In contrast, the confined ground state sees a greater fluctuation in the distribution of isotopes. As a result, the energy of the excited state is largely independent of the position of the donor; the energy of the ground state fluctuates more strongly with donor position. High-resolution Fourier transform infrared (FTIR) absorption spectroscopy of the $1s(A_1) \rightarrow 2p_0$ transition performed at a temperature of 1.5 K has revealed a linewidth of 0.033 cm^{-1} in isotopically enriched ^{28}Si with a phosphorus concentration of $N_P = 2 \times 10^{12} \text{ cm}^{-3}$, while the linewidth of the same transition in $^{\text{nat}}\text{Si}$ was found to be 0.082 cm^{-1} .³ If it is assumed that the transition is homogeneously broadened, then this corresponds to a lifetime of the $2p_0$ state of 161 ps for ^{28}Si and 65 ps for $^{\text{nat}}\text{Si}$. Time-domain pump-probe methods yield the lifetime of a particular state provided that pump and probe pulses are short with respect to the measured lifetime. For example, the lifetime of the $2p_0$ state in phosphorus-doped $^{\text{nat}}\text{Si}$ ($N_P = 2 \times 10^{15} \text{ cm}^{-3}$) was measured by this method to be $205 \pm 18 \text{ ps}$ at $\sim 5 \text{ K}$.¹ Taking into account the different types of samples, we are at liberty to assume a lifetime of ~ 160 to 200 ps for the $2p_0$ state in Si. This assumes that the transition is only homogeneously broadened. We show later that this is not the case.

One of the disputed issues is the effect of isotope broadening on the linewidth of intracenter optical transitions between energy levels and the lifetime of the states of shallow donors in Si. Recent theoretical calculations of the lifetime of the $2p_0$ state in Si (Refs. 4 and 5) differ significantly from what has been measured. Tsyplenkov *et al.* calculated the transition rate for nonradiative transitions from the $2p_0$ state to the $1s(E)$ and $1s(T_2)$ states.⁴ The model is semiempirical, because it constructs the envelope forms of the wave functions of the $1s$ states on the basis of experimental data on the energy of the eigenstate and uses the experimental data on electron-phonon interaction. Through this approach, the specific features of the short-range central cell potential of the donor are taken into account. They calculated the decay rates of the $2p_0 \rightarrow 1s(E)$, $1s(T_2)$ transitions, and it was shown that the lifetime of the $2p_0$ state is $\sim 40 \text{ ps}$.⁴ In contrast, Tyuterev *et al.* found the lifetime for the same donor state to be $\sim 1.1 \text{ ns}$.⁵ Their work is based on *ab initio* computation of the electron-phonon interaction in the framework of a density-functional perturbation approach applied to an ideal crystal. It combines the matrix elements of the electron-phonon coupling with the envelope function approximation for the impurity wave functions.

III. EXPERIMENTAL PROCEDURE

Dislocation-free Si crystals with natural isotopic composition and isotopically pure ^{28}Si were grown in the [100] direction by the float zone technique in an Ar atmosphere. The

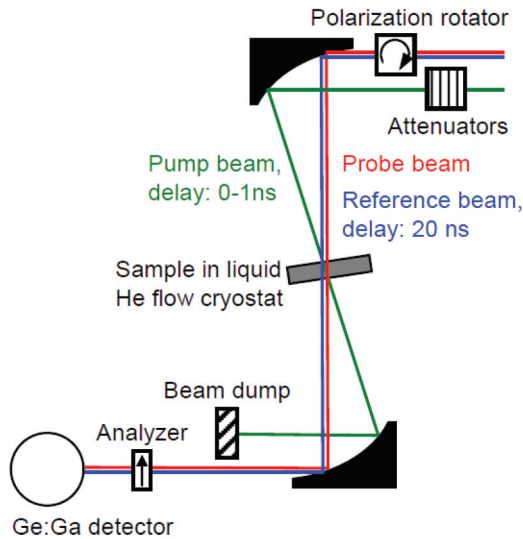


FIG. 2. (Color online) Scheme of the experimental setup.

starting material for the ^{28}Si crystal growth was produced in the framework of the Avogadro project.²⁴ The content of the ^{28}Si isotope in the crystal exceeds 0.99994; the oxygen and carbon concentrations measured by infrared spectroscopy are $\sim 4 \times 10^{14}$ and $\sim 2 \times 10^{14} \text{ cm}^{-3}$, respectively. The crystals were phosphorus-doped using gaseous phosphine. The doping concentrations of the Si crystals we use are $2 \times 10^{15} \text{ cm}^{-3}$ (^{28}Si) and $4 \times 10^{15} \text{ cm}^{-3}$ ($^{\text{nat}}\text{Si}$). Both samples were cut into rectangular parallelepipeds with an area of $7 \times 7 \text{ mm}^2$ and a thickness of 0.39 mm (^{28}Si) and 0.2 mm ($^{\text{nat}}\text{Si}$) and were chemically and mechanically polished with a wedge angle of 1° in order to avoid the effect of standing waves in the sample.

For the time-domain pump-probe measurements, we used the free electron laser for infrared experiments (FELIX) at the Foundation for Fundamental Research on Matter (FOM) in the Netherlands. FELIX emits macropulses of $\sim 6 \mu\text{s}$ with a repetition frequency of 10 Hz. Each macropulse consists of a train of micropulses with a duration of ~ 10 ps, separated by 40 ns. The experimental arrangement is a three-beam, balanced pump-probe technique described in Ref. 25 (Fig. 2). From the total power of the initial pulse, 5% is split off by a beam splitter. A second beam splitter separates this weak pulse into a probe beam and a reference beam. The relative delay between the strong pump and the weak probe beam can be varied between 0 and 1 ns. The reference beam is delayed by 20 ns with respect to the probe beam and measures the transmission of the unexcited sample. The three beams are focused onto the sample, and the transmitted probe and reference pulses are detected with a Ge:Ga photodetector. Its bias voltage is modulated at 25 MHz, which results in signals with the opposite sign for the probe and the reference beam. When no pump pulse is applied, the system is balanced; i.e., the integrating electronics shows a zero output signal.

The experiments were performed on the $1s(A_1) \rightarrow 2p_0$ transition. The measured relaxation rate of the $2p_0$ state includes contributions from the relaxation rates of the $1s(E)$ and $1s(T_2)$ states. However, this effect is small and can be neglected because of the fast relaxation from these states ($\sim 10^{11} \text{ s}^{-1}$).^{5,10} The peak pump power on the sample at the

$1s(A_1) \rightarrow 2p_0$ transition energy (34.1 meV) was estimated from the measured average output pulse energy to be ~ 60 nJ per micropulse. The pump power was attenuated up to 35 dB by a set of wire-grid attenuators.

The samples were strain-free mounted on a copper holder, which in turn was mounted to the cold finger of a liquid helium flow cryostat. The temperature of the sample was ~ 5 K. At this temperature, all donor-related electrons are in the $1s(A_1)$ ground state. When excited by the pump beam, electrons populate the state with an energy separation from the ground state equal to the pump photon energy. This nonequilibrium electron population relaxes into the ground state with a characteristic time T_1 . The change in transmission of the probe beam, which passes the Si sample, reflects changes in the optically induced nonequilibrium population of the excited state. By varying the time delay between pump and probe beams and measuring the transmittance through the sample as a function of this delay, we can determine T_1 .

IV. EXPERIMENTAL RESULTS AND DISCUSSION

The time-dependent transmittance of the probe beam was analyzed by a similar procedure to that described in Ref. 1. Prior to fitting, a constant offset was subtracted from the measured data. The offset is caused by nonperfect balancing, which is difficult to avoid even under ideal circumstances. We verified that it is an experimental artifact and not caused by an intracenter relaxation process by measuring the transmission signal when the FELIX wavelength is tuned to be out of resonance with any intracenter transition. We found that the offset is present in this situation as well. The data were fitted with a single exponential $C_0 \times \exp(t/T_1)$. As a control experiment, we determined the T_1 time of the $2p_0$ state in a $^{\text{nat}}\text{Si:P}$ reference sample. The result is $T_1 = 203 \pm 15$ ps, which is in excellent agreement with the lifetime of $T_1 = 205 \pm 18$ ps published by Vinh *et al.*¹

Examples of the change of the transmittance for the ^{28}Si crystal as a function of delay between pump and probe pulses are shown in Fig. 3 for different micropulse energies. For all pump powers, the decay is well described by a single exponential with the decay parameter $1/T_1$. In Fig. 4, the

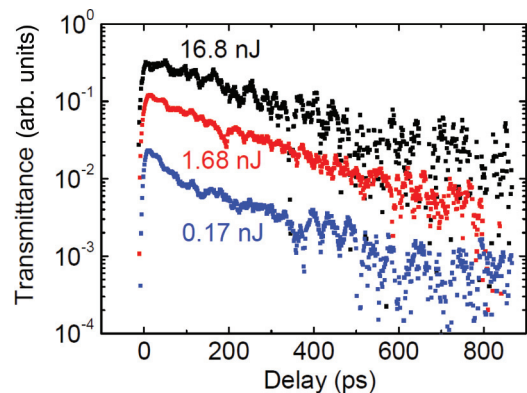


FIG. 3. (Color online) Transmittance of ^{28}Si induced by the pump beam as a function of delay between pump and probe pulse for different micropulse energies (given by the numbers in the figure). The micropulse length is 10 ps.

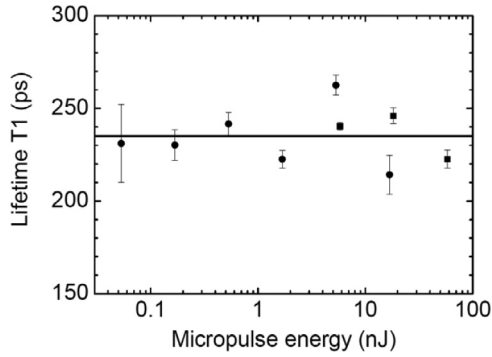


FIG. 4. Lifetime of the $2p_0$ state of ^{28}Si as determined from the exponential decay of the probe transmittance. The average value, as indicated by the straight line, is 235 ps.

values of T_1 are shown as a function of micropulse energy. They are independent of the pump energy and the mean value is $T_1 = 235 \pm 15$ ps. This value is 16% larger than the value of 203 ± 15 ps measured for $^{\text{nat}}\text{Si}:\text{P}$. It is instructive to compare these time-domain results with those extracted from the linewidth measurements of the $1s(A_1) \rightarrow 2p_0$ transition measured by FTIR spectroscopy.³ The linewidth in ^{28}Si is found to be 0.033 cm^{-1} , while for $^{\text{nat}}\text{Si}$ it is almost 2.5 times larger and amounts to 0.082 cm^{-1} . In comparison, the pump-probe measured lifetimes are different by only $\sim 16\%$. This shows that broadening caused by isotopic composition is predominantly an inhomogeneous process that affects the linewidth but not the lifetime.

Since the lifetime of the $2p_0$ state is determined by the emission of phonons, the different lifetimes of the $2p_0$ state in $^{\text{nat}}\text{Si}$ and ^{28}Si indicate that the electron-phonon interaction in both materials is different. One factor that affects the electron-phonon interaction is the nature of the intervalley scattering by g -LA and f -TA phonons, which determines the relaxation process of the $2p_0$ state. In contrast, g -TA phonons determine the decay of the $1s(E)$ and $1s(T_2)$ states. In an ideal Si crystal, the deformation potential is zero for electron intervalley transitions along high-symmetry directions in the Brillouin zone.⁵ The presence of isotopes lowers the symmetry of the crystal, allowing transitions with the emission of g -LA and f -TA phonons, in momentum directions that are otherwise forbidden. Thus, the deformation potential changes in $^{\text{nat}}\text{Si}$. This is emphasized by the peculiarities of the $2p_0$ state, which can be represented by an A_1 , an E , and a T_2 component—similar to the $1s$ ground state, although the components of the $2p_0$ state are spectrally not resolved. In case of a perfect Si crystal, electrons from the ground state can be directly photoexcited only into the A_1 and E components of the $2p_0$ state. However, scattering due to crystal imperfections such as different isotopes enables the transfer of electrons into the T_2 component. This opens an additional channel for relaxation and reduces the lifetime of the $2p_0$ state in $^{\text{nat}}\text{Si}$ compared to ^{28}Si . In a microscopic picture, one may consider the unit cells in ^{28}Si . These are all equal, and the displacement of neighboring unit cells caused by acoustic phonons is the same; i.e., there is no relative displacement of unit cells. In $^{\text{nat}}\text{Si}$, there is a significant probability that neighboring unit cells have different mass. Scattering by g -LA and g -TA phonons

leads to a relative displacement of unit cells with different mass, which in turn leads to additional strain, an increased deformation potential, and a reduced lifetime of the $2p_0$ state.

In the virtual-crystal approximation, the phonon frequencies of a monoatomic crystal are proportional to $\langle M \rangle^{-1/2}$, where $\langle M \rangle$ is the average mass of the isotopes in the crystal weighted by the corresponding isotopic abundance. Therefore, phonon frequencies of ^{28}Si are expected to be larger than those of $^{\text{nat}}\text{Si}$, and the phonon density of states is expected to shift toward higher frequencies. A manifestation of this effect is the shift of the peak in the Raman spectrum from 524 cm^{-1} for $^{\text{nat}}\text{Si}$ to 525 cm^{-1} for $^{28}\text{Si}:\text{P}$,¹⁸ which was also found for the Si samples of this paper. This also might affect the transitions involved in the decay of the $2p_0$ state. However, the shift is small; therefore, this contribution to the decrease of the lifetime in $^{\text{nat}}\text{Si}$ is expected to be negligible.

It is instructive to compare the results for n -type Si with those obtained for p -Si for which the effect of isotopic randomness has been studied experimentally and theoretically.^{26,27} It was found that the random distribution of the isotopes around the acceptor leads to a ground-state splitting and the shift of the center of mass of the transition energies causes a broadening. For Al, the broadening is $\sim 0.3 \text{ cm}^{-1}$, which is $\sim 2\%$ of the transition energy from the ground state to the next-higher excited state ($1\Gamma_8^-$). This indicates that the effect of isotopic randomness on the lifetime of a state is the qualitatively the same in p -type and n -type Si, although it differs quantitatively.

V. CONCLUSIONS

We have measured the lifetimes of the $2p_0$ state in ^{28}Si and $^{\text{nat}}\text{Si}$ using a terahertz pump-probe technique. The lifetime of ^{28}Si is found to be 16% larger than that of $^{\text{nat}}\text{Si}$. This is a much smaller difference than that found for the absorption linewidths of the $1s(A_1) \rightarrow 2p_0$ transition in low-doped Si crystals. From the time-domain measurements, it follows that linewidth broadening due to isotopic composition is an inhomogeneous process. The longer lifetime found for ^{28}Si compared to $^{\text{nat}}\text{Si}$ can be attributed to the higher symmetry of the ^{28}Si crystal and a less pronounced interaction of the $2p_0$ state, as well as the $1s(E)$ and $1s(T_2)$ states with the g -LA and f -TA phonons, which determine its lifetime. As a result, the lifetime of the $2p_0$ state in $^{\text{nat}}\text{Si}$ is shorter. Our results are in excellent agreement with previous lifetime measurements on $^{\text{nat}}\text{Si}$. However, there is a large discrepancy to theoretical calculations.^{4,5} In order to gain a quantitative understanding of the basic processes that govern the relaxation processes in impurity centers in semiconductors, it is desirable that the theoretical models are further improved. For this purpose, the well-investigated system Si:P represents an excellent model case.

ACKNOWLEDGMENTS

We acknowledge financial support from the United Kingdom Engineering and Physical Sciences Research Council Grants No. EP/E061265/1 and No. EP/H026622, the Nederlandse Organisatie voor Wetenschappelijk Onderzoek, and the Russian Foundation for Basic Research No. 11-02-00957. We thank the British Council and the Deutscher Akademischer Austausch Dienst (DAAD) for support through the Academic

Research Collaboration programm under Grant No. 1361 and DAAD under Project No. 50023075. We thank M. Wienold

and U. Böttger for assistance with the characterization of the samples.

*heinz-wilhelm.huebers@dlr.de

- ¹N. Q. Vinh, P. T. Greenland, K. Litvinenko, B. Redlich, A. F. G. van der Meer, S. A. Lynch, M. Warner, A. M. Stoneham, G. Aepli, D. J. Paul, C. R. Pidgeon, and B. N. Murdin, *Proc. Natl. Acad. Sci. USA* **105**, 10649 (2008).
- ²N. Q. Vinh, B. Redlich, A. F. G. van der Meer, C. R. Pidgeon, P. T. Greenland, S. A. Lynch, G. Aepli, and B. N. Murdin, *Phys. Rev. X* **3**, 011019 (2013).
- ³M. Steger, A. Yang, D. Karaiskaj, M. L. W. Thewalt, E. E. Haller, J. W. Ager III, M. Cardona, H. Riemann, N. V. Abrosimov, A. V. Gusev, A. D. Bulanov, A. K. Kaliteevskii, O. N. Godisov, P. Becker, and H.-J. Pohl, *Phys. Rev. B* **79**, 205210 (2009).
- ⁴V. V. Tsyplenkov, E. V. Demidov, K. A. Kovalevsky, and V. N. Shastin, *Semiconductors* **42**, 1016 (2008).
- ⁵V. Tyuterev, J. Sjakste, and N. Vast, *Phys. Rev. B* **81**, 245212 (2010).
- ⁶B. E. Kane, *Nature* **393**, 133 (1998).
- ⁷A. M. Stoneham, A. J. Fisher, and P. T. Greenland, *J. Phys. Condens. Matter* **15**, L447 (2003).
- ⁸M. Steger, K. Saeedi, M. L. W. Thewalt, J. J. L. Morton, H. Riemann, N. V. Abrosimov, P. Becker, and H.-J. Pohl, *Science* **336**, 1280 (2012).
- ⁹B. N. Murdin, J. Li, M. L. Y. Pang, E. T. Bowyer, K. L. Litvinenko, S. K. Clowes, H. Engelkamp, C. R. Pidgeon, I. Galbraith, N. V. Abrosimov, H. Riemann, S. G. Pavlov, H.-W. Hübers, and P. G. Murdin, *Nature Comm.* **4**, 1469 (2013).
- ¹⁰S. G. Pavlov, R. Kh. Zhukavin, E. E. Orlova, V. N. Shastin, A. V. Kirsanov, H.-W. Hübers, K. Auen, and H. Riemann, *Phys. Rev. Lett.* **84**, 5220 (2000).
- ¹¹S. G. Pavlov, H.-W. Hübers, J. N. Hovenier, T. O. Klaassen, D. A. Carder, P. J. Phillips, B. Redlich, H. Riemann, R. Kh. Zhukavin, and V. N. Shastin, *Phys. Rev. Lett.* **96**, 037404 (2006).
- ¹²M. Cardona and M. L. W. Thewalt, *Rev. Mod. Phys.* **77**, 1173 (2005).
- ¹³B. Andreas, Y. Azuma, G. Bartl, P. Becker, H. Bettin, M. Borys, I. Busch, M. Gray, P. Fuchs, K. Fujii, H. Fujimoto, E. Kessler, M. Krumrey, U. Kuetgens, N. Kuramoto, G. Mana, P. Manson, E. Massa, S. Mizushima, A. Nicolaus, A. Picard, A. Pramann, O. Rienitz, D. Schiel, S. Valkiers, and A. Waseda, *Phys. Rev. Lett.* **106**, 030801 (2011).
- ¹⁴R. K. Kremer, K. Graf, M. Cardona, G. Devyatykh, A. V. Gusev, A. M. Gibin, A. V. Inyushkin, A. Taldenkov, and H.-J. Pohl, *Solid State Comm.* **131**, 499 (2004).
- ¹⁵A. Gibin, G. Devyatykh, A. Gusev, R. Kremer, M. Cardona, and H.-J. Pohl, *Solid State Comm.* **133**, 569 (2005).
- ¹⁶E. Sozontov, L. X. Cao, A. Kazimirov, V. Kohn, M. Konuma, M. Cardona, and J. Zegenhagen, *Phys. Rev. Lett.* **86**, 5329 (2001).
- ¹⁷L. F. Lastras-Martínez, T. Ruf, M. Konuma, M. Cardona, and D. E. Aspnes, *Phys. Rev. B* **61**, 12946 (2000).
- ¹⁸F. Widulle, T. Ruf, A. Göbel, I. Silier, E. Schönherr, M. Cardona, J. Camacho, A. Cantarero, W. Kriegseis, and V. I. Ozhogin, *Phys. B* **263-264**, 381 (1999).
- ¹⁹A. K. Ramdas and S. Rodriguez, *Rep. Prog. Phys.* **44**, 1297 (1981).
- ²⁰C. Flensburg and R. F. Stewart, *Phys. Rev. B* **60**, 284 (1999).
- ²¹V. V. Tsyplenkov, K. A. Kovalevsky, and V. N. Shastin, *Semiconductors* **43**, 1410 (2009).
- ²²A. Griffin and P. Carruthers, *Phys. Rev.* **131**, 1976 (1963).
- ²³D. Karaiskaj, J. A. H. Stotz, T. Meyer, M. L. W. Thewalt, and M. Cardona, *Phys. Rev. Lett.* **90**, 186402 (2003).
- ²⁴P. Becker, H.-J. Pohl, H. Riemann, and N. Abrosimov, *Phys. Status Solidi A* **207**, 49 (2010).
- ²⁵S. A. Lynch, G. Matmon, S. G. Pavlov, K. L. Litvinenko, B. Redlich, A. F. G. van der Meer, N. V. Abrosimov, and H.-W. Hübers, *Phys. Rev. B* **82**, 245206 (2010).
- ²⁶D. Karaskaj, M. L. W. Thewalt, T. Ruf, M. Cardona, H.-J. Pohl, G. G. Deviatych, P. G. Sennikov, and H. Riemann, *Phys. Rev. Lett.* **86**, 6010 (2001).
- ²⁷D. Karaiskaj, G. Kirczenow, M. L. W. Thewalt, R. Buczko, and M. Cardona, *Phys. Rev. Lett.* **90**, 016404 (2003).